Inorganica Chimica Acta 376 (2011) 264–270

Contents lists available at ScienceDirect

Inorganica Chimica Acta

journal homepage: www.elsevier.com/locate/ica

DNA binding and nuclease activity of copper(II) complexes of tridentate ligands

Pankaj Kumar [a], Basudeb Baidya [a], Sumit Kumar Chaturvedi [b], Rizwan Hasan Khan [b], Debasis Manna [a,*], Biplab Mondal [a,*]

[a] Department of Chemistry, Indian Institute of Technology Guwahati, North Guwahati, Assam 781039, India
[b] Interdisciplinary Biotechnology Unit, Aligarh Muslim University, Aligarh 202002, India

ARTICLE INFO

Article history:
Received 22 March 2011
Received in revised form 7 June 2011
Accepted 10 June 2011
Available online 17 June 2011

Keywords:
Copper complexes
DNA
Binding
Cleavage

ABSTRACT

Two copper(II) complexes, **1** and **2** with $\mathbf{L_1}$ and $\mathbf{L_2}$ [$\mathbf{L_1}$ = 2-hydroxybenzyl(2-(pyridin-2-yl)ethylamine); $\mathbf{L_2}$ = 2-hydroxybenzyl(2-(pyridin-2-yl)methylamine)] ligands, respectively, have been synthesized and characterized. The interaction of both the complexes with DNA has been studied to explore their potential biological activity. The DNA binding properties of the complexes with calf thymus (CT) DNA were studied by spectroscopic titration. The complexes show binding affinity to CT DNA with binding constant (K_b) values in the order of 10^5 M^{-1}. Thermal denaturation and circular dichroism studies suggest groove binding of the complexes to CT DNA. Complexes also exhibit strong DNA cleavage activity in presence of reducing agents like 3-mercaptopropionic acid and β-mercaptoethanol. Mechanistic studies reveal the involvement of reactive hydroxyl radicals for their DNA cleavage activity.

1. Introduction

Irreversible modification of DNA by transition metal complexes has drawn considerable interest because of their potential applications as biological tools or as therapeutic agents. The chemical nuclease activity of these complexes is attributed to their ability to mediate oxidative damage to nucleobases and/or to the 2-deoxyribose moiety [1–18]. Knowledge of DNA binding parameters of these molecules is useful to explore their potential applications, since their binding mode could be associated with their ability to cause DNA damage [19–21]. Complexes of essential metals like copper and others are generally less toxic than of nonessential ones and some of them even have important cellular cytotoxic effects. In addition, high nucleobase affinity and comparatively strong Lewis acidity of copper(II) ion induce efficient DNA cleavage activity. As a result, copper complexes and their interactions with DNA have attracted great interest. Since the first report of $[Cu(phen)_2]^{2+}$ (phen = 1,10-phenanthroline) to display highly efficient oxidative cleavage of DNA, a considerable volume of the literature has been come out in this direction [22–29]. Recently, some of the mononuclear and polynuclear copper complexes with sulfonamides, pyridophenazine, ferrocenyl and others are reported to show strong chemical nuclease activities [30–42]. However, for an efficient DNA cleavage activity the metal ion has to be placed into the close proximity of DNA. It is known that the cations can bind to the DNA by attractive electrostatic interaction with the phosphate backbone, but these are rather weak in nature. Hence, strategies to develop copper(II) complexes which can bind DNA through intercalation or groove binding has been attracted a great attention.

At the same time, the target specificity is also an important parameter for the DNA cleavage and nuclease activity studies which can be attained by right choice of metal–ligand combination.

We have been systematically studying the DNA cleavage and nuclease activity of various copper(II) complexes of bidentate and tridentate ligands starting from noncytotoxic to moderately cytotoxic in nature. In this regard, for the present study two ligands, $\mathbf{L_1}$ and $\mathbf{L_2}$ [$\mathbf{L_1}$ = 2-hydroxybenzyl(2-(pyridin-2-yl)ethylamine; $\mathbf{L_2}$ = 2-hydroxybenzyl(2-(pyridin-2-yl)methylamine)] have been chosen considering that the phenolic-OH group may enhance the affinity of the complexes towards DNA binding through the formation of hydrogen bonding. On the other hand, because of the geometry of these complexes, they are likely to bind the polyanionic DNA via noncovalent outer-sphere coordination unlike the square planar complexes.

Here we report the syntheses of two copper(II) complexes, **1** and **2** with $\mathbf{L_1}$ and $\mathbf{L_2}$ [$\mathbf{L_1}$ = 2-hydroxybenzyl(2-(pyridin-2-yl) ethylamine; $\mathbf{L_2}$ = 2-hydroxybenzyl(2-(pyridin-2-yl)methylamine)] ligands, respectively (Fig. 1); single crystal structure of complex **2** and the interaction of both the complexes with DNA to explore their potential biological activity. The DNA binding properties of the complexes with calf thymus DNA (CT DNA) were studied by spectroscopic titration. The DNA conformational changes and cleavage activity of the complexes upon binding to the DNA were also studied in detail.

* Corresponding authors.
E-mail addresses: dmanna@iitg.ernet.in (D. Manna), biplab@iitg.ernet.in (B. Mondal).

0020-1693/$ - see front matter © 2011 Elsevier B.V. All rights reserved.
doi:10.1016/j.ica.2011.06.022

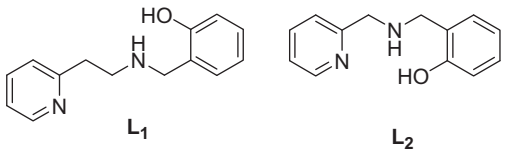

Fig. 1. Ligands used for the present study.

2. Experimental

2.1. Materials and methods

All reagents and solvents were purchased from commercial sources and were of reagent grade. The supercoiled (SC) pUC19 DNA (cesium chloride purified) was purchased from Bangalore Genie (India). Calf thymus (CT) DNA, ethidium bromide (EB), bovine serum albumin (BSA), 3-mercaptopropionic acid (MPA), β-mercaptoethanol (BME), bromophenol blue and xylene cyanol were from Sigma (USA). DMSO, KI, NaN_3, L-histidine were from Merck (Germany). Sodium dodecyl sulfate (SDS), glycerol, agarose (molecular biology grade) were purchased from SRL (India). Tris(hydroxymethyl)aminomethane–HCl (Tris–HCl) buffer was prepared using with Milli-Q water. UV–Vis spectra were recorded on a Perkin-Elmer Lambda 25 UV–Vis spectrophotometer. FT-IR spectra of the solid samples were recorded on a Perkin-Elmer spectrophotometer with samples prepared as KBr pellets. Solution electrical conductivity was checked using a Systronic 305 conductivity bridge. ^{1}H NMR spectra were obtained with a 400 MHz Varian FT spectrometer. Chemical shifts (ppm) were referenced either with an internal standard (Me_4Si) or to the residual solvent peaks. The X-band electron paramagnetic resonance (EPR) spectra were recorded on a JES-FA200 ESR spectrometer, at room temperature. Elemental analyses were obtained from a Perkin-Elmer Series II Analyzer. The magnetic moment of complexes is measured on a Cambridge Magnetic Balance.

2.2. X-ray crystallography

Single crystal was grown by slow diffusion followed by slow evaporation technique. The intensity data were collected using a Bruker SMART APEX-II CCD diffractometer, equipped with a fine focus 1.75 kW sealed tube Mo Kα radiation (λ = 0.71073 Å) at 273(3) K, with increasing ω (width of 0.3° per frame) at a scan speed of 3 s/frame. The SMART software was used for data acquisition. Data integration and reduction were undertaken with SAINT and XPREP software [43]. Multi-scan empirical absorption corrections were applied to the data using the program SADABS [44]. Structures were solved by direct methods using SHELXS-97 and refined with full-matrix least squares on F^2 using SHELXL-97 [45]. All nonhydrogen atoms were refined anisotropically. The hydrogen atoms were located from the difference Fourier maps and refined. Structural illustrations have been drawn with ORTEP-3 for Windows [46].

2.3. DNA binding experiments

The interaction of the complexes with calf thymus (CT) DNA was studied in Tris–HCl buffer (5 mM Tris–HCl, pH 6.8) at room temperature. CT DNA (ca. 375 μM NP) in the buffer medium gave a ratio of UV absorbance at 260 and 280 nm of 1.86:1, indicating that the DNA was sufficiently free from protein [47]. The concentration of DNA was measured from its absorption intensity at 260 nm using molar absorption coefficient (ε) value of 6600 M^{-1} cm^{-1} as reported [48]. The stock solutions of complexes were freshly prepared by first dissolving complexes in DMF and then diluted with buffer. The amount of DMF was kept less than 5% (by volume) for each set of experiment and has no effect on any experimental results.

Absorption titration experiments were performed by increasing the concentration of the CT DNA at constant (20 μM) complex concentration. Samples were initially equilibrated with CT DNA for 5 min before recording each spectrum. Proper correction was made to the absorbance of CT DNA. The strength of interactions of complexes to CT DNA was measured by monitoring the absorption intensity of the π–π^* transition band (~262 nm). The intrinsic binding constant (K_b) and the binding site size (s, per base pair) of the complexes to CT DNA were calculated by nonlinear least square analysis of the isotherm using the expression of Bard and co-workers [49] based on McGhee–von Hippel (MvH) model [50]

$$(\varepsilon_a - \varepsilon_f)/(\varepsilon_b - \varepsilon_f) = (b - (b^2 - 2K_b^2 C_t[\mathrm{DNA}]/s)^{1/2})2K_bC_t,$$

where $b = 1 + K_bC_t + K_b[\mathrm{DNA}]/2s$, ε_a is the extinction coefficient observed for the spectral band at a given DNA concentration, ε_f is the extinction coefficient of the complex in solution, ε_b is the extinction coefficient of the complex when fully bound to DNA, K_b is the equilibrium binding constant, C_t is the total complex concentration, [DNA] is the DNA concentration in nucleotides and s is the binding site size of the complexes in base pairs. The nonlinear least-square fit analysis was done using OriginLab software.

The apparent binding constant (K_{app}) values of the copper complexes to CT DNA were determined by ethidium bromide (EB) fluorescence displacement measurements using EB bound CT DNA solution in 5 mM Tris–HCl buffer (pH 6.8) at room temperature. The fluorescence intensities at 602 nm (526 nm excitation) of EB with increasing concentration of copper complexes were recorded. The K_{app} values were calculated from the equation: $K_{EB} \times [\mathrm{EB}] = K_{app} \times [\mathrm{complex}]$, where K_{EB} is the binding constant of EB ($K_{EB} = 1.0 \times 10^7$ M^{-1}), [EB] is the concentration of EB (1.3 μM) and [complex] is the concentration of the complex at 50% reduction of the emission intensity [2].

Thermal denaturation is known to cause an easily monitored hyperchromic effect in the absorption spectra of CT DNA (λ_{max}, 260 nm) [51]. Hence, the thermal denaturation of DNA in absence and presence of complexes were carried out by monitoring the absorbance of the CT DNA at 260 nm within the temperature range of 40–90 °C in 5 mM Tris–HCl buffer (pH 6.8). The experiments were carried out with the 3:1 molar ratio of the CT DNA to the complexes using Perkin-Elmer Lambda 25 spectrophotometer equipped with a peltier temperature-controller. The values of DNA melting temperature (T_m) were calculated from the derivative plot (dA_{260}/dT versus T) of the melting profile.

The circular dichroism (CD) spectroscopy was performed on a JASCO J-815 CD spectropolarimeter at room temperature. CD spectra of CT DNA in absence and presence of complexes in the 1:1 molar ratio of the CT DNA to the complexes were obtained in the wavelength range of 220–320 nm in 5 mM Tris–HCl buffer (pH 6.8). Each measurement was the average of three repeated scans, and the background was subtracted from all of the reagents by using a corresponding solution without CT DNA as a reference solution.

2.4. DNA cleavage experiments

The chemical nuclease activity of the complexes was monitored using supercoiled (SC) pUC19 DNA in presence of 3-mercaptopropionic acid (MPA, 500 μM) and β-mercaptoethanol (BME, 200 μM) as reducing agents and H_2O_2 (200 μM) as oxidizing agent in 50 mM Tris–HCl buffer containing 10% DMF and 50 mM NaCl (pH 6.8). The extent of cleavage of SC DNA (30 μM, 0.2 μg) to nicked circular (NC) and linear form by the complexes (50 μM) was measured by agarose gel electrophoresis. For mechanistic investigation

of the DNA cleavage reaction was performed in the presence of different additives like singlet oxygen quencher (NaN_3, 500 μM; L-histidine, 500 μM) and hydroxyl radical scavenger (DMSO, 4 μL; KI, 500 μM). The samples after incubation for 1.0 h at 37 °C under dark condition were added with the DNA loading buffer (25% bromophenol blue, 0.25% xylene cyanol FF and 30% glycerol). The gel electrophoresis was carried out in a dark room for 2.0 h at 40 V in a Tris-acetate EDTA (TAE) buffer using 1.0% agarose gel containing ethidium bromide (1.0 μg/ml). The gel images were captured by Bio-Rad gel documentation system and the extent of DNA cleavage was quantitatively calculated by ImageJ software. Due corrections were made for the low level of the nicked circular (NC) form present in the original SC DNA sample and for the low affinity of EB binding to SC compared to NC and linear forms of DNA.

2.5. Synthesis of the ligands and complexes

2.5.1. Synthesis of L_1

Salicylaldehyde (1.22 g, 10 mmol) in 25 ml methanol was taken in a 50 ml round bottomed flask fitted with a magnetic stir-bar and to this pyridine-2-ethylamine (1.22 g, 10 mmol) was added dropwise with constant stirring. Immediate formation of yellow precipitate of the corresponding Schiff base was observed and the stirring was continued for 1 h. The Schiff base was then filtered out and dried under reduced pressure to isolate as yellow solid (Yield: 1.60 g; ~70%). 1.30 g (5.75 mmol) of the Schiff base was then added in 20 ml methanol and reduced by the 2.5 equiv. of sodium borohydride. The colorless solution was dried under reduced pressure to afford a white mass. The mass was dissolved in 25 ml water and neutralized with dilute acetic acid. The organic product was then extracted from the aqueous solution using $CHCl_3$ (3× 20 ml portions); removal of the solvent under reduced pressure afforded pure L_1 ligand (Yield: 0.9 g; ~70%). Elemental analyses for $C_{14}H_{16}N_2O$: Calc. (%): C, 73.66; H, 7.06; N, 12.27. Found: C, 73.61; H, 7.07; N, 12.19%. ^{1}H NMR (400 MHz, $CDCl_3$): δ_{ppm} 2.98 (t, 2H), 3.06 (t, 2H), 3.97 (s, 2H), 6.77 (m, 2H), 6.93 (d, 1H), 7.12 (m, 3H), 7.57 (t, 1H), 8.49 (d, 1H). ^{13}C NMR (100 MHz, $CDCl_3$): δ_{ppm}, 37.30, 47.76, 52.52, 116.40, 118.97, 121.61, 122.68, 123.48, 128.43, 128.68, 136.65, 149.43, 158.42, 159.62.

2.5.2. Synthesis of L_2

The ligand L_2 was prepared from pyridine-2-methylamine (1.08 g, 10 mmol) and salicylaldehyde (1.22 g, 10 mmol) following the same procedure like L_1. Yield: (~75%). Elemental analyses $C_{13}H_{14}N_2O$: Calc. (%): C, 72.87; H, 6.59; N, 13.07. Found: C, 72.95; H, 6.61; N, 13.11%. ^{1}H NMR (400 MHz, $CDCl_3$): δ_{ppm}, 3.87 (s, 2H), 3.94 (s, 2H), 6.72 (t, 1H), 6.81 (d, 1H), 6.92 (d, 1H), 7.13 (m, 3H), 7.61 (d, 1H), 8.53 (d, 1H). ^{13}C NMR (100 MHz, $CDCl_3$): δ_{ppm}. 51.85, 53.08, 116.48, 119.16, 122.55, 122.84, 128.74, 128.86, 136.87, 149.44, 157.82, 158.22.

2.6. Synthesis of complex 1, $[Cu(L_1)](ClO_4)_2$

Copper(II) perchlorate hexahydrate, $[Cu(H_2O)_6](ClO_4)_2$ (2 g, 5.4 mmol) was dissolved in 10 ml of methanol and to this the ligand L_1 (2.46 g, 10.8 mmol) was added. The color of the solution was changed to green. The resulting mixture was stirred for 1 h at room temperature. The volume of the solution was then reduced to ~3 ml and kept in freezer for overnight to afford the complex **1** as green precipitate. It was then filtered off and washed with the small volume of cold methanol and dried under vacuum. Yield: 3.2 g (~82%). UV–Vis (acetonitrile): λ_{max}, 642 nm (ε = 240 M^{-1} cm^{-1}). FT-IR (KBr pellet): 1086, 1120, 764, 2928, 1483, 1258 cm^{-1}. Molar conductance: 240 S cm^{-1} mol^{-1}. Observed magnetic moment ≈1.66 BM.

2.7. Synthesis of complex 2, $[Cu(L_2)](ClO_4)_2$

Complex **2** was prepared from copper(II) perchlorate hexahydrate, $[Cu(H_2O)_6](ClO_4)_2$ (2 g, 5.4 mmol) and L_2 (2.31 g, 10.8 mmol) following the same procedure like complex **1**. Yield: 2.98 g (~80%). UV–Vis (acetonitrile): λ_{max}, 652 nm (ε = 121 M^{-1} cm^{-1}. FT-IR (KBr pellet): 1087, 1121, 753, 3254, 1433, 1614 cm^{-1}. Molar conductance: 248 S cm^{-1} mol^{-1}. The calculated magnetic moment is found to be 1.62 BM.

3. Results and discussions

The ligands, L_1 and L_2, were prepared by Schiff base reaction between the appropriate amine and aldehyde in methanol followed by the reduction of the Schiff base using sodium borohydride (Scheme 1) (see Section 2). The formation of the ligands was confirmed by various spectroscopic techniques as well as elemental analyses (see Section 2).

The complex **1** was prepared by stirring a methanol solution of $[Cu(H_2O)_6](ClO_4)_2$ with 2 equiv. of L_1 at room temperature for 1 h. After reducing the volume of the resulting deep blue solution, the solution was kept in freezer for overnight. The blue crystals of the complex were obtained from the mixture (Scheme 2).

The complex **2** was reported earlier [52]. The complex **2** was synthesized by the reaction of $[Cu(H_2O)_6](ClO_4)_2$ and L_2 following the same procedure. The formulation of the complexes has been supported by various spectroscopic analyses (Supporting information). The single crystal X-ray structure of complex **2** was determined. The ORTEP diagram is shown in Fig. 2. The crystallographic

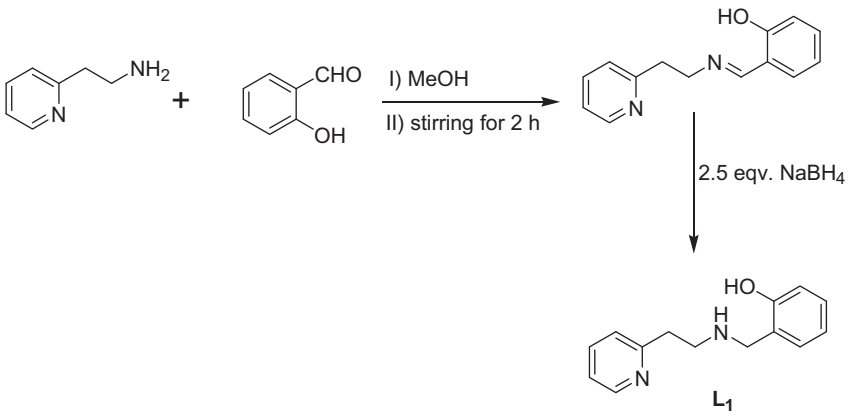

Scheme 1. Synthesis of ligand L_1.

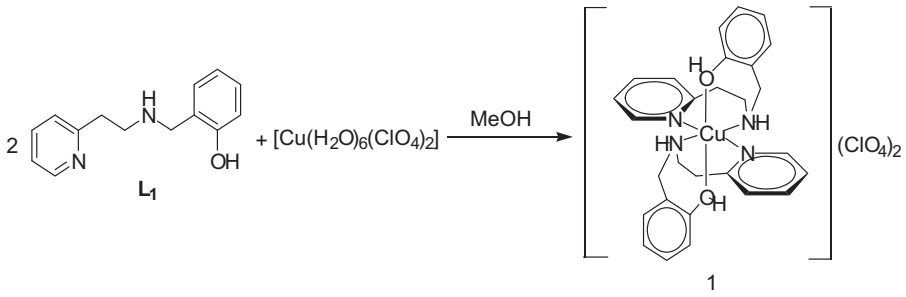

Scheme 2. Synthesis of complexes **1**.

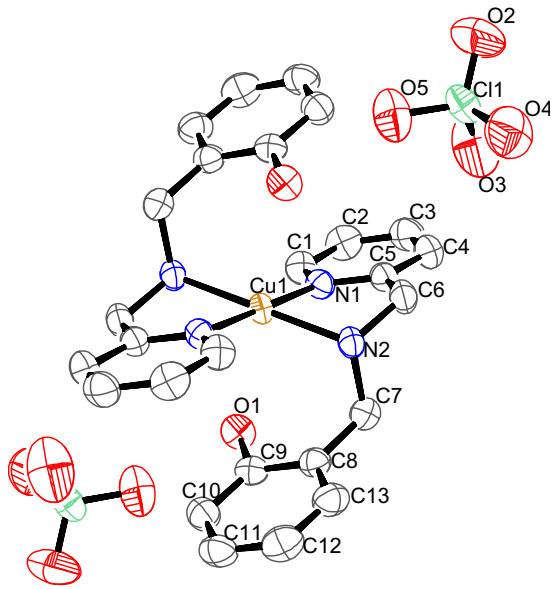

Fig. 2. ORTEP diagram for complex **2** (50% thermal ellipsoid plot). Hydrogen atoms are omitted for clarity.

Table 1
Crystallographic data for complex **2**.

Formula	$C_{26}H_{26}C_{l2}CuN_4O_{10}$
Molecular weight	688.96
Crystal system	monoclinic
Space group	$P\,2_1/n$
Temperature (K)	296(2)
Wavelength (Å)	0.71073
a (Å)	7.1126(5)
b (Å)	21.6213(15)
c (Å)	9.6947(7)
α (°)	90.00
β (°)	107.685(3)
γ (°)	90.00
V (Å^3)	1420.43(17)
Z	2
Density (mg m^{-3})	1.611
Absolute coefficient (mm^{-1})	1.021
Absolute correction	multi-scan
$F(0\,0\,0)$	706.0
Total number of reflections	3416
Reflections, $I > 2\sigma(I)$	2524
Maximum 2θ (°)	28.13
Index ranges	$-9 \leqslant h \leqslant 9$ $-28 \leqslant k \leqslant 27$ $-12 \leqslant l \leqslant 12$
Complete to 2θ (%)	98.2%
Refinement method	Full-matrix least-squares on F^2
Goodness-of-fit (GOF) on F^2	1.095
R indices [$I > 2\sigma(I)$]	0.0553
R indices (all data)	0.0698

data and a list of important bond angles and distances were given in Tables 1 and 2, respectively. The room temperature magnetic moment measurement showed one electron paramagnetism for both the complexes (1.66 and 1.62 BM for complex **1** and **2**, respectively). The complexes **1** and **2** displayed axial spectra in X-band EPR at room temperature in acetonitrile solvent which are characteristics of square planar Cu(II) complexes with $d_x^2 - d_y^2$ ground state ($g_{av} = 2.07$ and 2.14 for complexes **1** and **2**, respectively) [53,54]. Both the complexes were found to behave as 1:2 electrolyte in acetonitrile solution [Λ_M ($^{-1}$ cm^2 mol^{-1}), 247 and 259 for complexes **1** and **2**, respectively] [55].

3.1. DNA binding studies

The UV–Vis spectroscopy is used widely to study the binding of the metal complexes with DNA. It has been found that intercalation or electrostatic interaction between the metal complex and DNA leads to hypochromism; whereas hyperchromism indicates the break down of the secondary structure of DNA [56]. The UV–Vis absorption titrations have been employed to ascertain the DNA binding strength of complexes **1** and **2** by monitoring the changes in the absorption intensity of the ligand-centered bands around 262 nm. Fig. 3 illustrates the representative UV–Vis spectra for the binding of complexes in absence and presence of CT DNA (at a constant complex concentration, 20 μM) and the inset shows binding isotherm generated from the UV–Vis spectral data. With the increase in molar ratio (r) of DNA to complexes **1** and **2** (r = 0–3.6), the absorption intensity at ~262 nm increases by ~8- and 6-fold, respectively. This exceptionally strong hyperchromism, along with minor blue shift for complexes **1** and **2**, indicate strong interaction of the complexes with CT DNA mainly through groove binding [57]. It is known that the hyperchromicity of the UV absorbance band is caused by the unwinding of the double helix as well as its unstacking and the concomitant exposure of the bases; whereas, red- or blue-shift indicates that the complex may have some effect on DNA [11,57,58]. To compare the binding parameters quantitatively, the intrinsic equilibrium binding constant (K_b) for the complexes **1** and **2** (shown in Table 3) have been determined to be 8.56×10^4 M^{-1} and 7.15×10^4 M^{-1}, and the binding site size (s) to be 0.79 and 0.77 (b.p.), respectively (Table 3). The higher binding constant values could be due to the presence of aromatic rings, which might facilitate the interaction of the complexes with the DNA bases through noncovalent π–π interaction. The lower value of s ($s < 1$) suggests groove binding and/or surface aggregation of the complexes on DNA, which also correlates with the hyperchromicity of the UV-absorptions in presence of higher DNA concentrations (Fig. 3) [59].

The binding strength of the complexes to CT DNA has been further verified by measuring apparent DNA binding constants (K_{app}) from ethidium bromide (EB) fluorescence displacement assay

Table 2
Selected bond lengths (Å) and bond angles (°) for complex **2**.

Angle (°)		Bond length (Å)	
N1–Cu1–N2	81.6(1)	Cu1–N1	2.022(2)
N1–Cu1–O1	97.43(8)	Cu1–N2	2.037(2)
N1–Cu1–N1	180.0(1)	Cu1–O1	2.635(3)
N1–Cu1–N2	98.4(1)	Cu1–N1	2.022(2)
N1–Cu1–O1	82.57(8)	Cu1–N2	2.037(2)
N2–Cu1–O1	86.52(9)	Cu1–O1	2.635(3)
N2–Cu1–N1	98.4(1)	N1–O5	1.346(3)
N2–Cu1–N2	180.0(1)	N1–C1	1.338(4)
N2–Cu1–O1	93.48(9)	N2–C6	1.493(4)
O1–Cu1–N1	82.57(8)	N2–C7	1.491(5)
O1–Cu1–N2	93.48(9)		
O1–Cu1–O1	180.00(7)		
N1–Cu1–N2	81.6(1)		
N1–Cu1–O1	97.43(8)		
N2–Cu1–O1	86.52(9)		

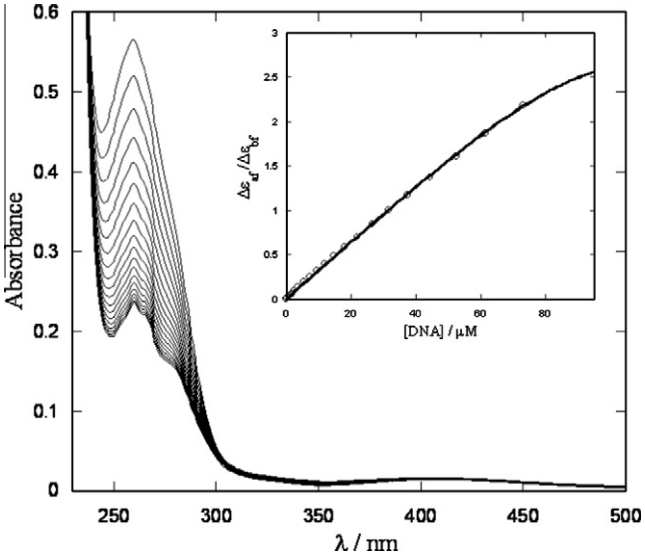

Fig. 3. Representative absorption spectra of complex **1** (20 μM) in Tris–HCl buffer (pH 6.8) with the increase in molar ratio of DNA to complex (0–3.6) at room temperature. The inset shows the nonlinear least square fit of $\Delta\varepsilon_{af}/\Delta\varepsilon_{bf}$ vs. [DNA] using the expression of Bard and co-workers based on McGhee–von Hippel model.

Table 3
DNA binding parameters for complexes.

	1	2
K_b[a] (M^{-1}) [s]	8.56 (±0.3) × 10^4, [0.79]	7.15 (±0.3) × 10^4, [0.77]
K_{app}[b] (M^{-1})	1.76 (±0.3) × 10^5	8.45 (±0.2) × 10^4
ΔT_m[c] (°C)	+1.37	−2.7
K_{BSA}[d] (M^{-1})	3.3 (±0.3) × 10^4	1.3 (±0.1) × 10^4

[a] Intrinsic equilibrium binding constant from UV–Vis absorption titration.
[b] Apparent DNA binding constant from fluorescence displacement assay.
[c] Change in DNA melting temperature of CT DNA.
[d] Bovine serum albumin (BSA) binding constant from fluorescence spectral measurements.

(Fig. 4). EB is known to show reduced emission intensity in buffer solution due to solvent quenching, and an enhancement of the emission intensity when EB intercalatively binds to dsDNA [60]. The competitive binding of the complexes to DNA has been measured from the extent of reduction of the EB emission intensity at 602 nm. The inset shows the binding isotherm generated from the fluorescence spectra of EB. The K_{app} values indicate that complex **1** binds better than the complex **2** (Table 3). The small difference in apparent binding constant values also in consistent with the intrinsic binding constants. Thus, both intrinsic and apparent binding parameters clearly show that complexes **1** and **2** strongly interact with CT DNA.

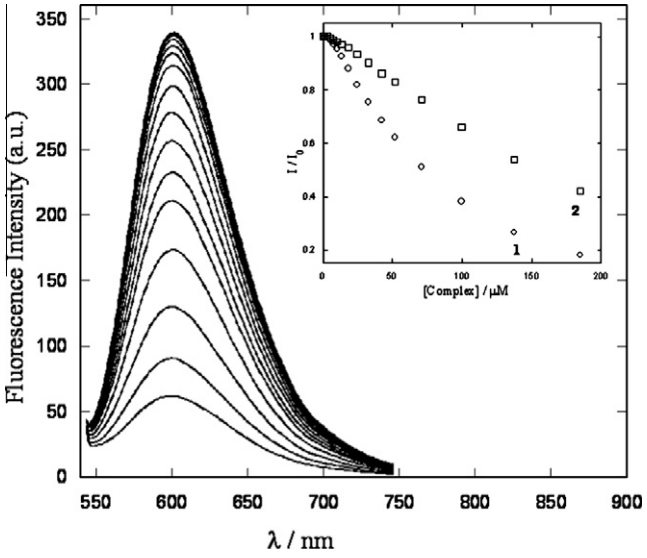

Fig. 4. Representative fluorescence emission spectra of DNA-EB in Tris–HCl buffer (pH 6.8) with the increase in molar ratio of complex **1** to DNA (0–3.4) at room temperature. The inset shows the plot of I/I_0 vs. [complex] for fluorescence quenching curves of DNA-EB by complexes **1** and **2**.

Thermal behavior of DNA in the presence of the metal complexes has also been studied. The dsDNA at its melting temperature unwinds to give a single strand DNA, resulting in the increase of absorbance at 260 nm. In general, intercalation of small molecules to dsDNA is associated with high melting temperatures. A minor shift in the CT DNA T_m value in presence of complexes **1** and **2**, respectively, confirm predominant groove binding mode of the complexes (Fig. 5a and Table 3). The higher ΔT_m value for complex **1** (+1.37 °C) than complex **2** (−2.7 °C) could be due to the extended flexibility of the ligand in complexes **1** compare to **2**, which has been reflected in binding parameters.

For further understanding of the DNA structural changes in presence of complexes and to reconfirm the mode of interactions the CD studies have been performed. The positive absorption band at 274 nm and the negative one at 245 nm in the CD spectrum are due to the base stacking and the right-handed helicity of B-DNA, respectively [56,61]. The CD spectrum of CT DNA in presence of complex **1** at 1:1 molar ratio shows an increase in positive band (98%) and decreases in negative band (37%) with a blue shift of 3 nm and 1 nm, respectively, compared to the only CT DNA. Under similar condition complex **2** shows an increase in positive band (81%) and decrease in negative band (18%) with a blue shift of 1 nm for positive band only. These changes in CD spectrum of CT DNA indicate strong conformational changes by the complexes. The major change at 274 nm absorption band clearly indicates that both the complexes interact with dsDNA through groove and/or surface and decreases the helicity of the dsDNA. The larger CD spectral changes by **1** than **2** are in correlation with their DNA binding parameters.

3.2. DNA cleavage study

To investigate whether the DNA binding and DNA conformational changing properties of the complex **1** and **2** are associated with further pharmacological activities, chemical nuclease activity assay have been performed. The cleavage activity of complexes to-

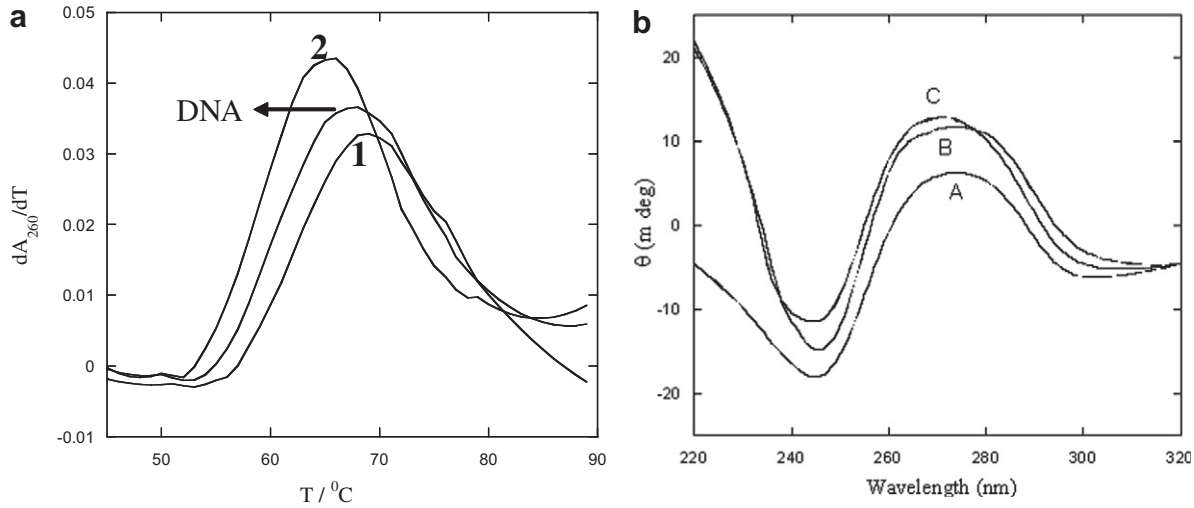

Fig. 5. (a) Derivative plot of thermal denaturation of CT DNA (150 μM) only and in presence of complexes (50 μM) in Tris–HCl buffer (pH 6.8). (b) Circular dichroism spectra of (A) CT DNA only, (B) CT DNA in presence of complex **2** and (C) CT DNA in presence of complex **1** in Tris–HCl buffer (pH 6.8) at room temperature. [complex] = 150 μM, [DNA] = 150 μM.

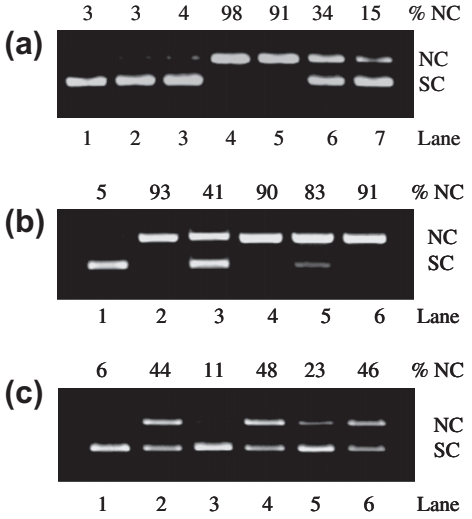

Fig. 6. (a) Representative gel electrophoresis diagram showing the chemical nuclease activity of the complexes (50 μM) using SC pUC19 DNA (30 μM, 0.2 μg) in presence of 3-mercaptopropionic acid (MPA, 500 μM) and β-mercaptoethanol (BME, 200 μM): lane 1, DNA control; lane 2, DNA + MPA; lane 3, DNA + BME; lane 4, DNA + **1** + MPA; lane 5, DNA + **1** + BME, lane 6, DNA + **2** + MPA; lane 7, DNA + **2** + BME. (b) and (c) Representative gel electrophoresis diagram showing the mechanistic aspects of chemical nuclease activity of SC pUC19 DNA (30 μM, 0.2 μg) by the complexes **1** and **2**, respectively, in presence of singlet oxygen quencher like, NaN_3 (500 μM), L-histidine (500 μM) and hydroxyl radical scavengers like DMSO (6 μL), KI (500 μM): lane 1, DNA control; lane 2, DNA + **1/2** + MPA; lane 3, DNA + **1/2** + MPA + DMSO; lane 4, DNA + **1/2** + MPA + NaN_3; lane 5, DNA + **1/2** + MPA + KI; lane 6, DNA + **1/2** + MPA + L-histidine.

wards SC pUC19 DNA has been investigated by measuring the extent of formation of nicked circular (NC) DNA (Fig. 6a) in the presence of reducing agents. Complex **1** found to be highly active forming ~98% and ~91% NC in presence of reducing agents like 3-mercaptopropionic acid (MPA) or β-mercaptoethanol (BME), respectively. Complex **2** also exhibits good chemical nuclease activity showing formation of ~34% and ~15% NC in presence of reducing agents like MPA and BME, respectively. The extent of DNA cleavage by the complexes as observed from the agarose gel electrophoresis also follows their DNA binding propensity. The complexes in presence of oxidizing agent like H_2O_2 also exhibit

Table 4
Chemical nuclease activity of SC pUC19 DNA by the complexes in presence of various additives.

Complex	% NC DNA					
	DNA only	Complex + MPA	+DMSO[a]	+NaN_3[b]	+KI[c]	+L-histidine[d]
1	5	93	41	90	83	91
2	6	44	11	48	23	46

[complex] = 50 μM.
[a] DMSO = 6 μL.
[b] [NaN_3] = 500 μM.
[c] [KI] = 500 μM.
[d] [L-Histidine] = 500 μM.

similar cleavage activity (Supporting information). Control experiments using only reducing agents like MPA and BME, oxidizing agents like H_2O_2 or the complexes alone (Supporting information) have not shown appreciable DNA cleavage under similar experimental conditions.

To understand the basis of chemical nuclease activity of the complexes in presence of reducing agents we have systematically investigated the mechanistic aspects using various additives. The addition of hydroxyl radical scavengers like DMSO, KI and the singlet oxygen quenchers like NaN_3, L-histidine in absence of any reducing agent have almost modest or no effect on DNA cleavage activity, respectively (Table 4).

This indicates their noninvolvement in DNA cleavage activity. Whereas, in presence of reducing agents only the hydroxyl radical scavengers showed significant inhibitory effect in the chemical nuclease activity (Fig. 6b and c). This mechanistic data suggest that the DNA cleavage reaction of the complexes in presence of MPA, presumably, proceeds via hydroxyl radical pathway.

4. Conclusions

The synthesis and structural characterization of Cu(II) complexes **1** and **2** were carried out with an aim to study their DNA binding and nuclease activity. Both the complexes effectively interact with CT DNA through groove binding mode resulting in strong conformational changes of the CT DNA. The chemical nuclease

activity study indicates that **1** has stronger cleavage activity than **2**. The mechanistic studies indicate that the hydroxyl radicals are the main driving force and the extent of DNA cleavage in presence of hydroxyl radicals, is governed to a large extent by their DNA binding mode and propensity. This work presents a good overall correlation between DNA binding and DNA cleavage activity of the complexes. Further biological studies are beyond the scope of this investigation. The results are of importance towards further designing and developing Cu(II) based complexes and systematic assessment of DNA binding, cleavage activity for their potential applications as therapeutic agents.

Acknowledgements

The authors acknowledge their sincere gratitude to the Department of Chemistry, Central Instrumentation Facility, Indian Institute of Technology Guwahati, India. The authors are also thankful to the DST and DBT, India for financial support. DST, India for the FIST funded X-ray diffractometer.

Appendix A. Supplementary material

Electronic Supplementary Information (ESI) available: all the spectroscopic characterisation for the ligands, complexes, ORTEP diagram for complex **1** and gel electrophoresis data are included.

Supplementary data associated with this article can be found, in the online version, at doi:10.1016/j.ica.2011.06.022.

References

[1] M. Pitié, C.J. Burrows, B. Meunier, Nucleic Acids Res. 28 (2000) 4856.
[2] B. Maity, M. Roy, S. Saha, A.R. Chakravarty, Organometallics 28 (2009) 1495.
[3] R. Tawa, D. Gao, M. Takami, Y. Imakura, K.-H. Lee, H. Sakurai, Bioorg. Med. Chem. 6 (1998) 1003.
[4] M.E. Branum, A.K. Tipton, S. Zhu, L. Que Jr., J. Am. Chem. Soc. 123 (2001) 1898.
[5] J.-C. Francois, T. Saison-Behmoaras, C. Barbier, M. Chassignol, N.T. Thuong, C. Héléne, Proc. Natl. Acad. Sci. USA 86 (1989) 9702.
[6] M.P. Fitzsimons, J.K. Barton, J. Am. Chem. Soc. 119 (1997) 3379.
[7] R. Hettich, H.-J. Schneider, J. Am. Chem. Soc. 119 (1997) 5638.
[8] B.C. Bales, M. Pitié, B. Meunier, M.A. Greenberg, J. Am. Chem. Soc. 124 (2002) 9062.
[9] J.A. Cowan, Curr. Opin. Chem. Biol. 5 (2001) 634.
[10] A. Sreedhara, J.D. Freed, J.A. Cowan, J. Am. Chem. Soc. 122 (2000) 8814.
[11] Y.L. Song, Y.T. Li, Z.Y. Wu, J. Inorg. Biochem. 102 (2008) 1691.
[12] C. Sissi, F. Mancin, M. Gatos, M. Palumbo, P. Tecilla, U. Tonellato, Inorg. Chem. 44 (2005) 2310.
[13] A. Nomura, Y. Sugiura, J. Am. Chem. Soc. 126 (2004) 15374.
[14] X.Q. Chen, X.J. Peng, J.Y. Wang, Y. Wang, S. Wu, L.Z. Zhang, T. Wu, Y.K. Wu, Eur. J. Inorg. Chem. (2007) 5400.
[15] T. Gupta, S. Dhar, M. Nethaji, A.R. Chakravarty, Dalton Trans. (2004) 1896.
[16] E. Boseggia, M. Gatos, L. Lucatello, F. Mancin, S. Moro, M. Palumbo, C. Sissi, P. Tecilla, U. Tonellato, G. Zagotto, J. Am. Chem. Soc. 126 (2004) 4543.
[17] L.T. Ellis, D.F. Perkins, P. Turner, T.W. Hambley, Dalton Trans. (2003) 2728.
[18] K.M. Deck, T.A. Tseng, J.N. Burstyn, Inorg. Chem. 41 (2002) 669.
[19] C.H. Ng, K.C. Kong, S.T. Von, P. Balraj, P. Jensen, E. Thirthagiri, H. Hamada, M. Chikira, Nucleic Acids Res. 28 (2000) 4856.
[20] A. Sancar, G.B. Sancar, Annu. Rev. Biochem. 57 (1998) 29.
[21] S.S. David, S.D. Williams, Chem. Rev. 98 (1998) 1221.
[22] D.R. Graham, L.E. Marshall, K.A. Reich, D.S. Sigman, J. Am. Chem. Soc. 102 (1980) 5419.
[23] S.P. Foxon, T. Phillips, M.R. Gill, M. Towrie, A.W. Parker, M. Webb, J.A. Thomas, Angew. Chem., Int. Ed. 46 (2007) 3686.
[24] A. Neves, M. Lanznaster, A.J. Bortoluzzi, R.A. Peralta, A. Casellato, E.E. Castellano, P. Herrald, M.J. Riley, G. Schenk, J. Am. Chem. Soc. 129 (2007) 7486.
[25] C. Metcalfe, J.A. Thomas, Chem. Soc. Rev. 32 (2003) 215.
[26] M.J. Clarke, F. Zhu, D.R. Frasca, Chem. Rev. 99 (1999) 2511.
[27] B.M. Zeglis, V.C. Pierre, J.K. Barton, Chem. Commun. (2007) 4565.
[28] J. Reedijk, Proc. Natl. Acad. Sci. USA 100 (2003) 3611.
[29] A. Ghosh, A. Mandoli, D.K. Kumar, N.S. Yadav, T. Ghosh, B. Jha, J.A. Thomas, A. Das, Dalton Trans. (2009) 9312.
[30] T.-S.A. Tseng, J.N. Burstyn, Chem. Commun. (2008) 6209.
[31] M. Tian, H. Ihmels, E. Brötz, Dalton Trans. (2010), doi:10.1039/c0dt00238k.
[32] T. Afrati, A.A. Pantazaki, C.D. Samara, C. Raptopoulou, A. Terzis, D.P. Kessissoglou, Dalton Trans. 39 (2010) 765.
[33] A. Bencini, E. Berni, A. Bianchi, C. Giorgi, B. Valtancoli, D.K. Chand, H.-J. Schneider, Dalton Trans. (2003) 793.
[34] K.J. Humphreys, K.D. Karlin, S.E. Rokita, J. Am. Chem. Soc. 123 (2001) 5588.
[35] K.J. Humphreys, K.D. Karlin, S.E. Rokita, J. Am. Chem. Soc. 124 (2002) 6009.
[36] K.J. Humphreys, A.E. Johnson, K.D. Karlin, S.E. Rokita, J. Biol. Inorg. Chem. 7 (2002) 835.
[37] K.J. Humphreys, K.D. Karlin, S.E. Rokita, J. Am. Chem. Soc. 124 (2002) 8055.
[38] J. Chen, X. Wang, Y. Shao, J. Zhu, Y. Zhu, Y. Li, Q. Xu, Z. Guo, Inorg. Chem. 46 (2007) 3306.
[39] J.L. García-Giménez, G. Alzuet, M. González-Álvarez, M. Liu-González, A. Castiñeiras, J. Borrás, J. Inorg. Biochem. 103 (2009) 243.
[40] M. González-Álvarez, G. Alzuet, J. Borrás, B. Macías, A. Castiñeiras, Inorg. Chem. 42 (2003) 2992.
[41] Y. Zhao, J. Zhu, W. He, Z. Yang, Y. Zhu, Y. Li, J. Zhang, Z. Guo, Chem. Eur. J. 12 (2006) 6621.
[42] C.H. Ng, K.C. Kong, S.T. Von, P. Balraj, P. Jensen, E. Thirthagiri, H. Hamada, M. Chikira, Dalton Trans. (2008) 447.
[43] SMART, SAINT and XPREP, Siemens Analytical X-ray Instruments Inc., Madison, Wisconsin, USA, 1995.
[44] G.M. Sheldrick, SADABS: Software for Empirical Absorption Correction, University of Gottingen, Institut fur Anorganische Chemieder Universitat, Tammanstrasse 4, D-3400 Gottingen, Germany, 1999–2003.
[45] G.M. Sheldrick, SHELXS-97, University of Gottingen, Germany, 1997.
[46] L.J.J. Farrugia, Appl. Crystallogr. 30 (1997) 565.
[47] J. Marmur, P. Doty, J. Mol. Biol. 3 (1961) 585.
[48] M.E. Reichmann, S.A. Rice, C.A. Thomas, P. Doty, J. Am. Chem. Soc. 76 (1954) 3047.
[49] M.T. Carter, M. Rodriguez, A.J. Bard, J. Am. Chem. Soc. 111 (1989) 8901.
[50] J.D. Mcghee, P.H.V. Hippel, J. Mol. Biol. 86 (1974) 469.
[51] D.L. Nelson, M.M. Cox, Lehninger, Principles of Biochemistry, fourth ed., W.H. Freeman, and Company, New York, 2005.
[52] A. Neves, C.N. Verani, M.A. de Brito, I. Vencato, A. Mangrich, G. Oliva, D.D.H.F. Souza, A.A. Batista, Inorg. Chim. Acta 290 (1999) 207.
[53] A.W. Addison, H.M.J. Hendriks, J. Reedijk, L.K. Thompson, Inorg. Chem. 20 (1981) 103.
[54] T.N. Sorrell, D.L. Jameson, Inorg. Chem. 21 (1982) 1014.
[55] B. Mondal, V.G. Puranik, G.K. Lahiri, Inorg. Chem. 41 (2002) 5831.
[56] M. Chauhan, K. Banerjee, F. Arjmand, Inorg. Chem. 46 (2007) 3072.
[57] F. Mancin, P. Scrimin, P. Tecilla, U. Tonellato, Chem. Commun. 20 (2005) 2540.
[58] T. Hirohama, Y. Kuranuki, E. Ebina, T. Sugizaki, H. Arii, M. Chikira, P.T. Selvi, M. Palaniandavar, J. Inorg. Biochem. 99 (2005) 1205.
[59] M.S.A. Begum, S. Saha, M. Nethaji, A.R. Chakravarty, J. Inorg. Biochem. 104 (2010) 477.
[60] J.B. Lepecq, C. Paoletti, J. Mol. Biol. 27 (1967) 87.
[61] K. Karidi, A. Garoufis, A. Tsipis, N. Hadjiliadis, H. den Dulk, J. Reedijk, Dalton Trans. 7 (2005) 1176.